Inclusion of Randomness into SPH Simulations

MARTIN HUŠEK, FILIP HOKEŠ, JIŘÍ KALA, PETR KRÁL
Faculty of Civil Engineering, Institute of Structural Mechanics
Brno University of Technology
Veveří 331/95, 602 00 Brno
CZECH REPUBLIC
husek.m@fce.vutbr.cz, hokes.f@fce.vutbr.cz, kala.j@fce.vutbr.cz, kral.p@fce.vutbr.cz,
http://www.fce.vutbr.cz

Abstract: The complexity of numerical simulations is increasing alongside the growing need to capture the behaviour of real-world processes as well as possible. A frequent problem is the inclusion of the randomness factor in numerical simulations in order to better reflect the results of experiments. In cases when the material used in experiments shows signs of heterogeneity, it is also advisable to introduce it in the numerical model. The inclusion of heterogeneity can take place in several ways, though this of course always depends on the numerical method chosen. This contribution describes a procedure which can be used to implement material heterogeneity within the numerical code of the Smoothed Particle Hydrodynamics (SPH) method. The whole algorithm is explained using the example of a cylindrical concrete body striking a solid base. Aspects which need to be maintained to ensure algorithm functionality are described, too. As it is relatively difficult to implement the initial singularities of the crack type into the SPH method, a procedure is described at the end of the article which can be used to implement initial cracks to simulations using a described algorithm. The results of the simulations show that the described algorithms can be used successfully.

Key-Words: Heterogeneity; Smoothed Particle Hydrodynamics; support domain; fracture; randomness; concrete.

1 Introduction

The original idea in the very foundations of structure designing and related domains consisted in creating a simple and robust concept. With the progress of time, simple outlines gradually became more complicated, eventually reaching a stage where a mere pencil with a sheet of paper had ceased to suffice. Interestingly, at present we are often faced with efforts to design structures as simple as reasonably possible; after being completed, however, such structures may not necessarily be the simplest ones in terms of their behavior and the presumptions of structural mechanics [1-3].

In concrete structures, the material heterogeneity offers a new dimension of complexity. Concrete, as the mixture of a concrete additive, a cement binder, and water, does not constitute a regular structure from any perspective or at any scale; with respect to this fact, not even the behaviour of the given structures can be assumed to remain identical in all cases. The introduced randomness is further multiplied by the type of load, which is invariably comprised in structural mechanics analyses [4-6].

In real-world conditions, countless loading tests can be carried out, and the rates of occurrence of an effect enable us to presume the most probable result of the series of tests to follow. However, numerical analyses and simulations, using common computational techniques such as the Finite Element Method (FEM), Finite Difference Method (FDM), or Smoothed Particle Hydrodynamics method (SPH), will not provide divergent results even with an infinite number of computations unless special add-ons are applied.

In simulations where concrete-based materials are involved, we always encounter the problem of what material model is to be used [7,8]. The results obtained from the varied models and their modified versions can differ fundamentally. Yet it is not advisable to introduce the heterogeneity directly into the description of the material model, mainly due to the increasing complexity of the operations and the lack of knowledge concerning the sensitivities of the model's individual parameters before running the actual computation [9,10]. For example, in the case of the FEM, a material model would have to be generated for each finite element to ensure that the material heterogeneity is contained in the numerical model.

A hitherto scarcely employed option consists in implementing the heterogeneity directly into the source code of the numerical method; however, there still remain the questions of whether this approach can be used to define the random behavior of the monitored area, or the heterogeneity, and whether

such numerical treatment can be further interconnected and explained using a real concrete structure. Numerical attenuation is utilized in fracture mechanics simulations, where the FEM often finds effective application. As the material model is the same in the entire monitored area, the finite element geometry can be modified such that any failure is immediately localizable at a pre-selected point (for example, via notching on a concrete beam). In high-speed loading, however, the FEM does not offer a suitable solution [11,12].

Conversely, the attractivity of the SPH approach intensifies with the increasing loading speed; yet we also need to note that, in the case of the SPH, there is no physical mesh to interconnect the individual particles, and a mere change in the configuration of the particles may not provide the desired results (in fact, this type of action may even cause adverse effects, including the formation of numerical cracks) [13,14].

The paper presents a procedure to introduce the heterogeneity into the source code of the SPH method in such a manner that the individual particles appear like concrete additive, binder, or water particles to create a random material structure, which then generates diverse simulation results. The contribution also defines the restrictions to be observed. Further, a simple fracture mechanics experiment where a concrete disc strikes a rigid surface and is deformed is simulated.

For easier orientation within the text, the contribution is divided into chapters which will explain the individual steps of the procedure of heterogeneity implementation. Chapter 2 describes the essential idea of the SPH method, including the equations which are modified by the presented algorithm. In this context, issues concerning the size of the support domain in SPH simulations are reviewed. Chapter 3 describes a numerical experiment in which the heterogeneity implementation procedure is tested. It also includes a warning regarding compliance with certain limitations in order to guarantee the functionality of the algorithm. Chapter 4 explains the individual steps of the algorithm together with an example of its output for a specific case. Chapter 5 is divided into two main sections that show the results of the numerical experiment while illustrating the functionality of the algorithm, including its use for the implementation of initial cracks.

2 Essential formulation of the SPH

The formulation of the SPH method is often divided into two key steps. The first step is the *integral representation* of field functions, and the second is *particle approximation*. The concept of the integral representation of a function $f(\boldsymbol{x})$ used in the SPH method starts from the following identity:

$$f(\boldsymbol{x}) = \int_{\Omega} f(\boldsymbol{x}')\delta(\boldsymbol{x}-\boldsymbol{x}')d\boldsymbol{x}' \tag{1}$$

where f is a function of the three-dimensional position vector $\boldsymbol{x}$, and $\delta(\boldsymbol{x}-\boldsymbol{x}')$ is the Dirac delta function given by

$$\delta(\boldsymbol{x}-\boldsymbol{x}') = \begin{cases} +\infty & \boldsymbol{x} = \boldsymbol{x}' \\ 0 & \boldsymbol{x} \neq \boldsymbol{x}' \end{cases} \tag{2}$$

In (1), Ω is the volume of the integral that contains $\boldsymbol{x}$. Equation (1) implies that a function can be represented in an integral form. Since the Dirac delta function is used, the integral representation in (1) is exact or rigorous as long as $f(\boldsymbol{x})$ is defined and continuous in Ω [13]. If the Delta function $\delta(\boldsymbol{x}-\boldsymbol{x}')$ is replaced by a smoothing function $W(\boldsymbol{x}-\boldsymbol{x}', h)$, the integral representation of $f(\boldsymbol{x})$ is given by

$$f(\boldsymbol{x}) \approx \int_{\Omega} f(\boldsymbol{x}')W(\boldsymbol{x}-\boldsymbol{x}', h)d\boldsymbol{x}' \tag{3}$$

where W is the so-called smoothing function and h is the smoothing length defining the influence area of the smoothing function W. Note that as long as W is not the Dirac delta function, the integral representation in (3) can only be an approximation [13].

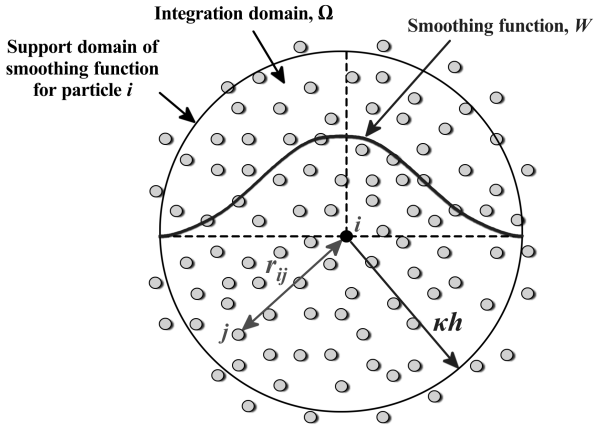

Fig. 1. The particle approximations using particles within the support domain of the smoothing function W for particle i.

The continuous integral representations concerning the SPH integral approximation in (3) can be converted into discretized forms of summation over all the particles in the support domain shown in Fig. 1. The corresponding discretized process of

summation over the particles is commonly known as particle approximation.

If the infinitesimal volume $d\boldsymbol{x}'$ in (3) at the location of particle j is replaced by the finite volume of the particle ΔV_j that is related to the mass of the particles m_j by

$$m_j = \Delta V_j \rho_j \tag{4}$$

where ρ_j is the density of particle j (= 1, 2,…, N) in which N is the number of particles within the support domain of particle j, then the continuous SPH integral representation for $f(\boldsymbol{x})$ can be written in the following form of discretized particle approximation [13]:

$$\begin{aligned} f(\boldsymbol{x}) &\approx \int_{\Omega} f(\boldsymbol{x}')W(\boldsymbol{x}-\boldsymbol{x}',h)d\boldsymbol{x}' \\ &\approx \sum_{j=1}^{N} f(\boldsymbol{x}_j)W(\boldsymbol{x}-\boldsymbol{x}_j,h)\Delta V_j \\ &\approx \sum_{j=1}^{N} f(\boldsymbol{x}_j)W(\boldsymbol{x}-\boldsymbol{x}_j,h)\frac{1}{\rho_j}(\rho_j \Delta V_j) \\ &\approx \sum_{j=1}^{N} f(\boldsymbol{x}_j)W(\boldsymbol{x}-\boldsymbol{x}_j,h)\frac{1}{\rho_j}(m_j) \end{aligned} \tag{5}$$

or just

$$f(\boldsymbol{x}_i) \approx \sum_{j=1}^{N} \frac{m_j}{\rho_j} f(\boldsymbol{x}_j)W(\boldsymbol{x}_i-\boldsymbol{x}_j,h) \tag{6}$$

Equation (6) states that the value of a function at particle i is approximated using the average of those values of the function at all the particles in the support domain of particle i weighted by the smoothing function shown in Fig. 1.

2.1 Problem with the support domain

The extent of the support domain is defined according to Fig. 1 as the size of the generally variable parameter h, which is called the smoothing length. Parameter h can also be multiplied by constant κ. Particles which are inside the support domain attributable to particle i are called neighbouring particles. If the resultant value of the product κh in each time step of the numerical simulation is the same, there can be the decrease in the number of neighbouring particles and thus also the decrease in the accuracy of the solution due the effect of excessive deformations (i.e. during the mutual divergence of the SPH particles). It is advisable to change the size of the support domain during the calculation in such a way that the number of neighbouring particles is constant.

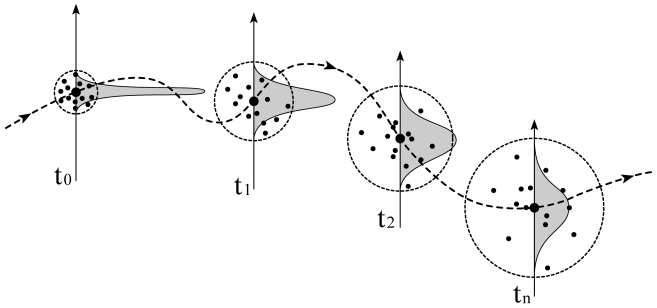

Fig. 2. Evolution of the support domain during the simulation. Smoothing length increases when particles separate from each other.

There are many ways to dynamically develop h so that the number of neighbouring particles remains relatively constant. In 1989, Benz [14] suggested a method of developing the smoothing length. This method uses the time derivative of the smoothing function in terms of the continuity equation

$$\frac{dh}{dt} = -\frac{1}{d}\frac{h}{\rho}\frac{d\rho}{dt} = \frac{1}{d}h\,\nabla\cdot\boldsymbol{v} \tag{7}$$

where d is the number of dimensions and $\nabla\cdot\boldsymbol{v}$ is the divergence of the flow. This means that the smoothing length increases when particles separate from each other and reduces when the concentration of particles is significant; see Fig. 2. It varies in order to keep the same number of particles in the neighbourhood. Equation (7) can be discretized using SPH approximations and calculated with other differential equations in parallel [13].

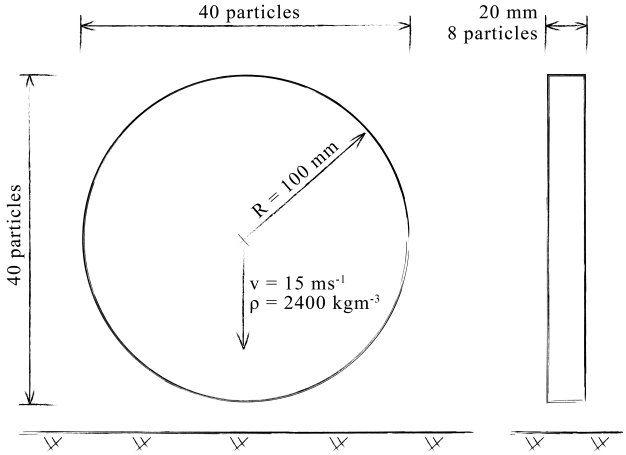

Fig. 3. A diagram of the experiment.

3 Experiment set up and restrictions

Before characterizing the procedure applied to introduce the material heterogeneity into the numerical model, a brief description of the simulated

experiment, whose diagram is presented in Fig. 3, is provided. The scheme shows a cylindrical concrete body striking a rigid surface at the speed of 15 ms^{-1}. As one of the preconditions for the functionality of the introduced algorithm consists in regular initial particle distribution, the cylinder was discretized with 8 particles in the depth and 40 particles in the height and width.

The particles were arranged to form a regular, grid-based (and therefore not a radial) field, as also indicated in Fig. 6. The simulations involved 10,112 SPH particles in total and were performed via the LS-DYNA program [15]. The Continuous Surface Cap Model (CSCM) was chosen as the material model of concrete to be used [16,17]. Table 1 shows the parameters employed in the simulations.

Table 1

The material parameters for the CSCM model.

Mass density, ρ_c (kgm^{-3})	2400
Compressive strength, f_c (MPa)	43.10
Initial shear modulus, G (GPa)	12.92
Initial bulk modulus, K (GPa)	14.15
Poisson's ratio, v_c	0.18
Fracture energy, G_F (Jm^{-2})	83.25
Maximum aggregate size, a_g (mm)	8

3.1 Essential restrictions

A drawback of the SPH method lies in the effect of the initial particle distribution. The imperfect regularity of the particles, such as that observed in the presence of particle clusters with interparticle distances markedly different from the rest of the model, may result in the formation of numerical (false) cracks. Even though the problem can be tackled through introducing the smoothing function defined in the material coordinates (a Lagrangian kernel), such a procedure would cause the analyzed model to lose the capability of solving excessive deformations. When, however, using the smoothing function defined in the spatial coordinates (an Eulerian kernel), we need to suitably change the size of the smoothing length to ensure that the number of particles in the support domain ideally remains constant during the entire simulation [14].

As the simulated experiment was a high-speed one and the discretization of the monitored body via the SPH particles was regular, the smoothing function defined in the spatial coordinates, namely, an Eulerian kernel, was selected.

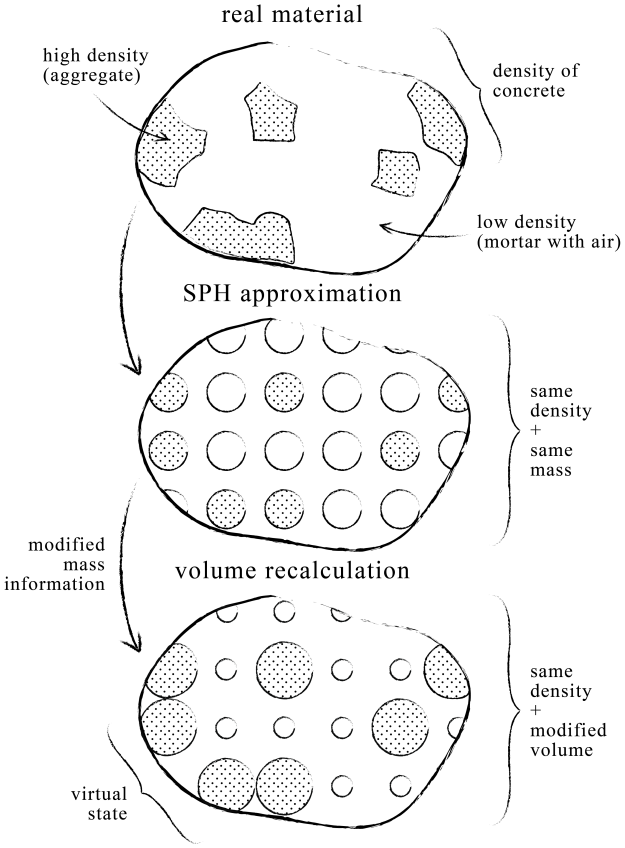

Fig. 4. Including the numerical heterogeneity in the SPH model.

4 Numerical heterogeneity

The implementation of the material heterogeneity was performed via modifying the weight value function of the individual SPH particles; in other words, the particle mass m_j included in (6) was modified. Further, the same density value was preserved in all the particles, meaning that – with respect to the validity of (4) – the volume assigned to the individual particles was virtually modified (enlarged/reduced).

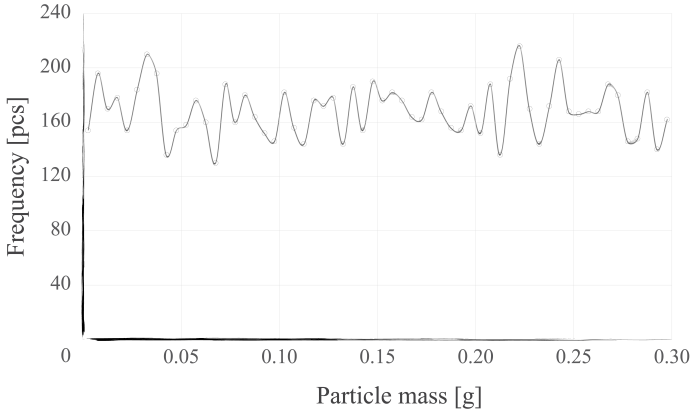

Fig. 5. The mass distribution function of specimen #1.

However, due to the necessity to maintain the best possible particle distribution regularity (an identical smoothing length for all the particles), the initial particle distribution was generated for the state where all the particles are assigned the same volume ΔV_j. This operation is graphically represented in Fig. 4.

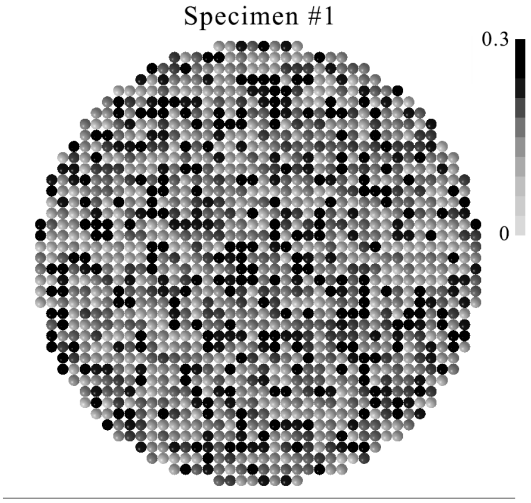

Fig. 6. The mass distribution of specimen #1 (units in g).

4.1 Mass distribution

As the individual SPH particles had to be assigned various masses, it was necessary to build the entire distribution algorithm upon the precondition of a constant weight of the resulting body. The algorithm can nevertheless satisfy the conditions of any distribution function (including, for example, the normal, uniform, or Poisson distribution variants). For the actual testing, the uniform distribution of the occurrence of masses was selected, and the relevant occurrence rate resembled that shown in Fig. 5.

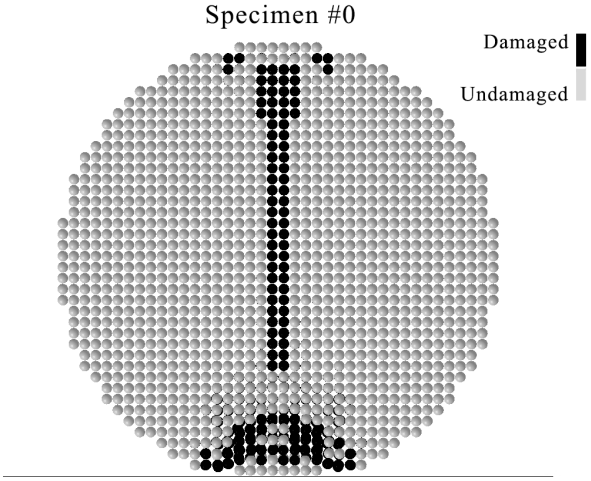

Fig. 7. The deformation of the homogeneous model.

The reason for choosing uniform distribution consisted in testing the computational stability. The properties of the smoothing function enable the SPH method to suppress or highlight the heterogeneities contained in a computational procedure [13]. By another definition, the sensitivity of the computational stability in the presence of particles with almost zero mass (such as air pores in concrete) was tested.

Fig. 6 demonstrates one of the tested samples with representation of the masses. Before running a computation, the pattern of Fig. 5 was re-generated to create a modified model according to the algorithm in Fig. 4, with a result similar to that shown in Fig. 6.

5 Results

This section compares the behavior of the modified models with that of the homogeneous one (no heterogeneity introduced, all particles exhibit the same mass and density).

The gray-marked portions of the images invariably represent crackless material, whereas the black sectors stand for failures. All the results were captured at the same instant of time.

The homogeneous model, Fig. 7, clearly exhibits a crushed region at the zone of contact with the rigid surface. The localized main crack symmetrically passes through the center of the model, and it does not tend to open any further during the simulation. With respect to the material homogeneity, the concrete cylinder shows very high resistance to complete failure.

Fig. 8 presents disrupted models with the introduced material heterogeneity. A unique mass distribution pattern was generated for each specimen, as is obvious from Fig. 5. Importantly, Fig. 8 indicates that the introduction of the heterogeneity renders the models more sensitive to not only accidental disruption but also failure in general. In this context, another finding consists in the identification of multiple main cracks developing simultaneously. The value of parameter $\kappa = 1.0$ was used for the results in Fig. 8. In other words, the extent of the support domain was exactly according to (7).

5.1 Influence of the κ parameter

As the results of SPH simulations strongly depend on the size of the support domain, the effect of the κ value when heterogeneity is introduced was also examined.

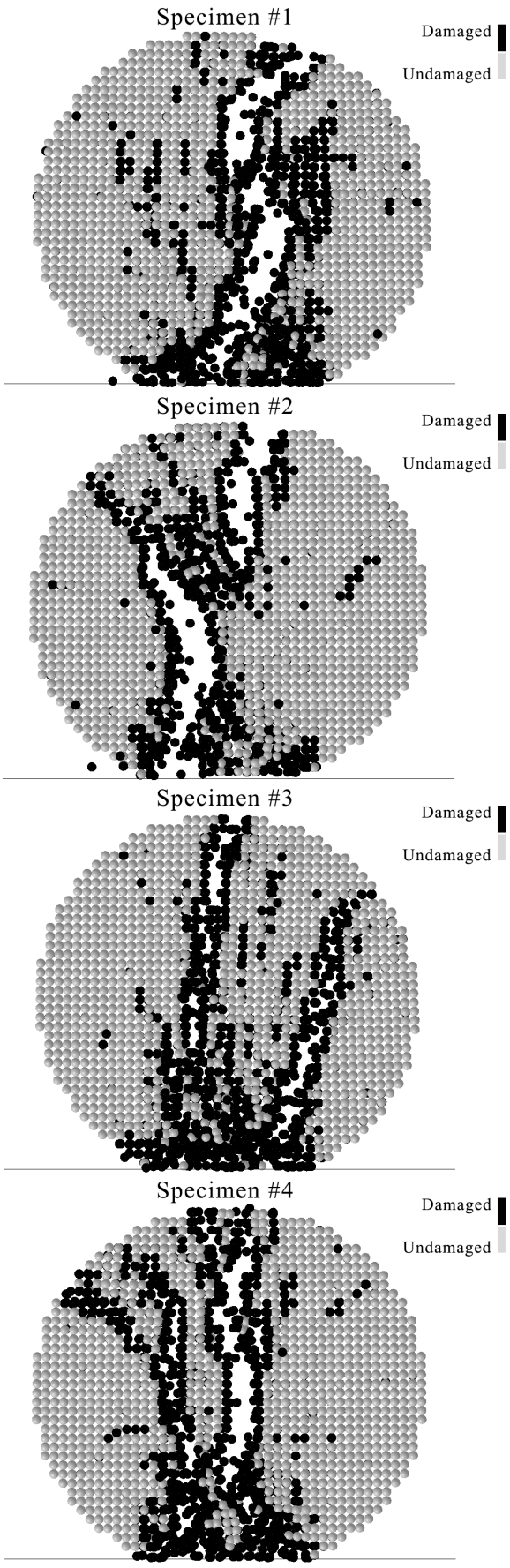

Fig. 8. The deformation of the heterogeneous models. Value of $\kappa = 1.0$.

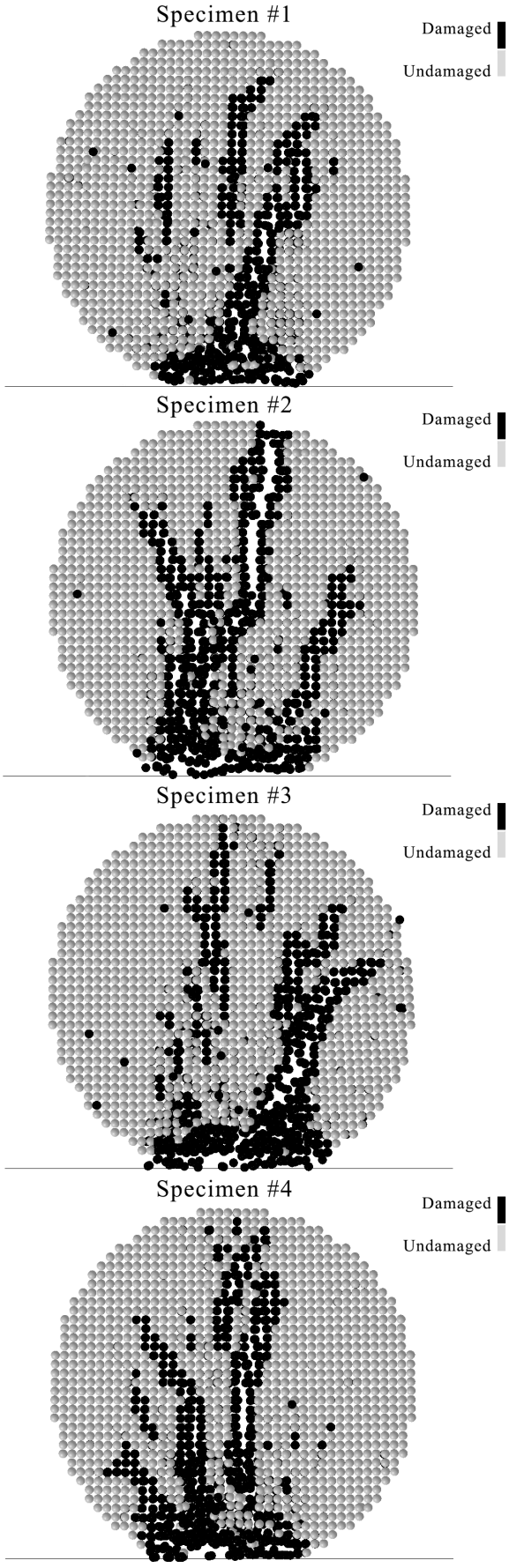

Fig. 9. The deformation of the heterogeneous models. Value of $\kappa = 1.5$.

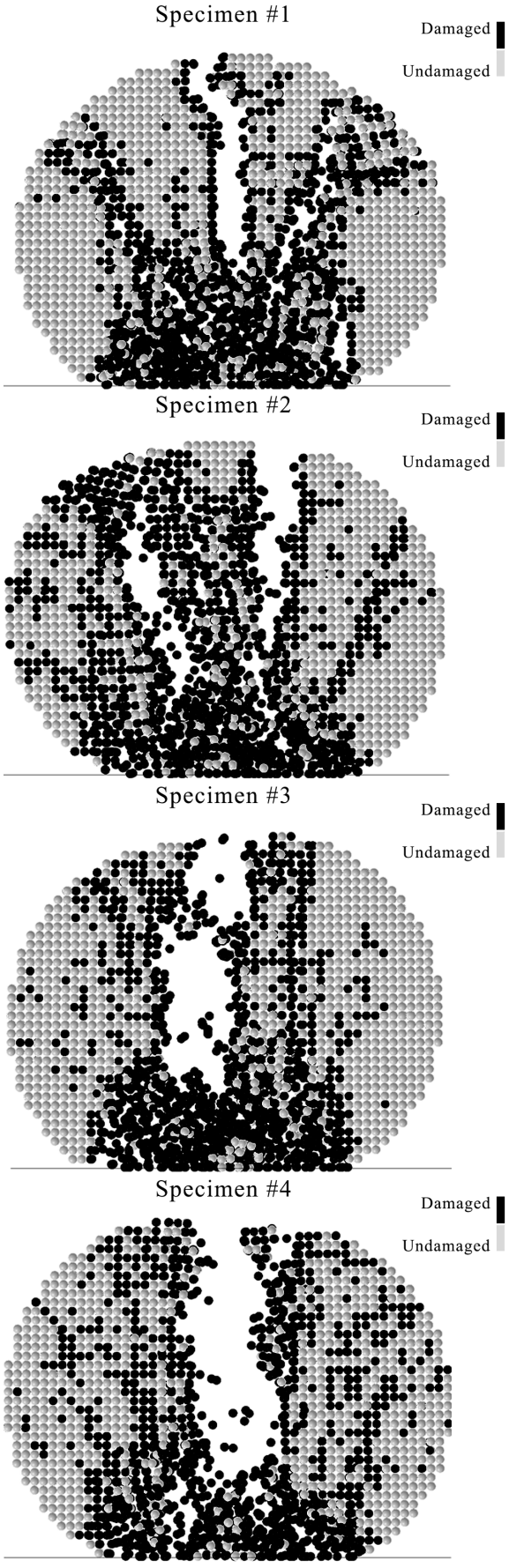

Fig. 10. The deformation of the heterogeneous models. Value of $\kappa = 0.7$.

Thanks to its smoothing functions (see Fig. 1), the SPH method can either highlight or suppress heterogeneity. The results of the simulations with different κ values are shown in Figs. 9. and 10.

As can be seen in Fig. 9, when the $\kappa = 1.5$, the heterogeneity of the material slowly vanishes. No more main cracks are created – quite the opposite. There is only one main crack and small cracks accumulate in its surroundings. However, there is still extensive deformation in the area of contact with the solid base.

In the case of the results in Fig. 10 when the $\kappa = 0.7$, again only one main crack was created. However, a larger failure clearly occurs both in the area of the main crack and in the area where the disc makes contact with the solid base. This shows that heterogeneity is a lot clearer than in the case of the results in Figs. 8 and 9. It is also clear from the results that the values of contact forces will differ. This is a result of the different sizes of the deformation zones, and thus the different sizes of the kinetic energy transformed into plastic deformation. The κ value must thus ideally be chosen with regard to the results of the experiment; see [18].

5.2 Initial crack simulation

In the case of the SPH method, it is difficult to simulate initial cracks in the model. This is caused by the fact that two SPH particles in close proximity to each other cannot be divided numerically. In other words, non-symmetrical smoothing functions would have to be created in the whole area of the crack, which can be very problematic.

One of the possible procedures for the simulation of initial cracks in the SPH model is the use of the previously mentioned algorithm with the introduction of numerical heterogeneity. Basically, the crack is simulated by particles which are assigned zero weight. In the sense of (6), this means that the area with particles simulating the crack will not be interlaid smoothly with smoothing functions but rather will be interlaid with a certain singularity representing the drop in smoothing functions.

Fig. 11 shows three examples with an introduced initial crack or with pre-fractured material. Again, failure results were tested. The aim of the simulation was to connect the failure with the introduced initial crack. The results are shown (with depicted weight) in Fig. 12 and (with a depicted damage parameter) in Fig. 13.

It is clear from the results in Fig. 12 that the cracks which occur undergo initial failure. This is proof of the apparent weakening of the material being simulated by particles with zero weight. The results

in Fig. 13 show that the main crack undergoes initial failure, which is accompanied only by tiny cracks in its surroundings.

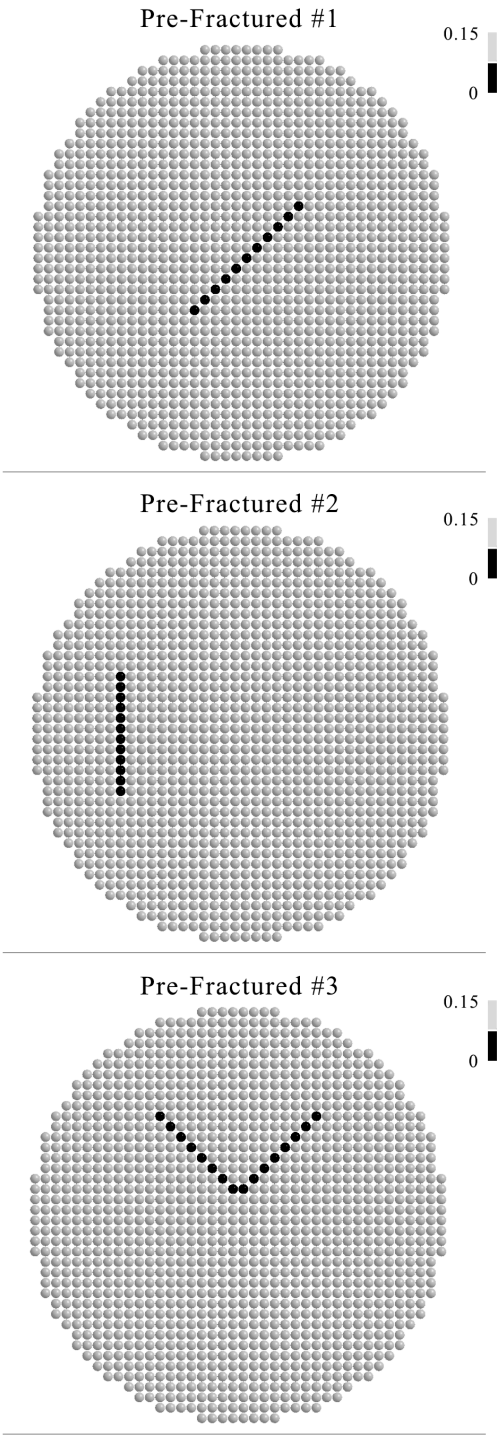

Fig. 11. Mass of particles with simulated pre-fractured material (units in g).

5.3 Further observation

The presented results show the functionality of the algorithm and also the idea behind the whole procedure. It was already mentioned in Chapter 4.1 that the mass of the SPH particles also reached zero values.

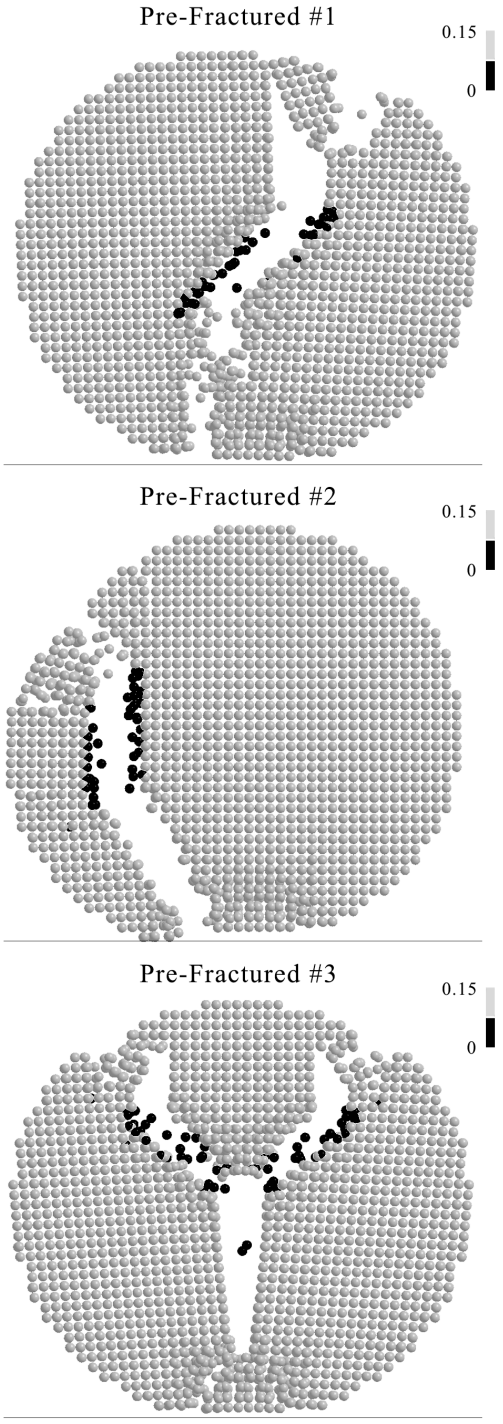

Fig. 12. The deformation of the pre-fractured models with plotted mass (units in g).

Even though the computational stability of the SPH method was confirmed, a problem may arise in the interaction between the base – FEM shell elements – and SPH particles. This interaction was investigated using a simple penalty-based contact algorithm in which the stiffness of the virtual spring, $k(t)$, between

the interacting master and slave elements plays an important role. The SPH particles are considered to be slave nodes and the FEM elements to be master segments. In the majority of cases, it is sufficient to define the stiffness as

$$k(t) = \alpha m \left(\frac{1}{\Delta t_c(t)} \right)^2 \tag{8}$$

where $k(t)$ is the stiffness of the virtual spring, α is a factor with which the stiffness of the virtual spring can be decreased/increased, m is the mass of the SPH particle which is in contact, and $\Delta t_c(t)$ is the current time step of the simulation. Unfortunately, it is clear that this procedure cannot be used in the case when the mass of the SPH particle $m \rightarrow 0$. One solution is to base the stiffness on the bulk modulus, K. For FEM shell elements the stiffness of the virtual spring $k(t)$ could then be expressed as

$$k(t) = \frac{\alpha K A}{\max(\text{shell diagonal})} \tag{9}$$

where α is a factor with which the stiffness of the virtual spring can be decreased/increased, K is the averaged bulk modulus of the interacting materials, and A is the face area of the FEM shell element which is in contact. There were no other numerical problems or instabilities during the simulations.

6 Conclusion

The paper discusses a simple procedure for introducing numerical heterogeneity into SPH-based models. Interestingly, such numerical heterogeneity stems from a real property of concrete-based materials. The principles of the relevant algorithm and the conditions that, if satisfied, enable to avoid numerical cracks, which are unrelated to the numerical heterogeneity are also characterized. As the whole algorithm for the heterogeneity implementation of a material is based on the modification of the weight value function of individual SPH particles, it is not necessary to generate a great number of material models as is often the case with other methods – on the contrary, only one is sufficient. This greatly decreases the requirements for the initial stages of the calculation. Moreover, it is very easy to introduce various heterogeneity fields which are related to any distribution function via the direct modification of the SPH source code. It can be said that another advantage of the presented method is its simplicity and transparency.

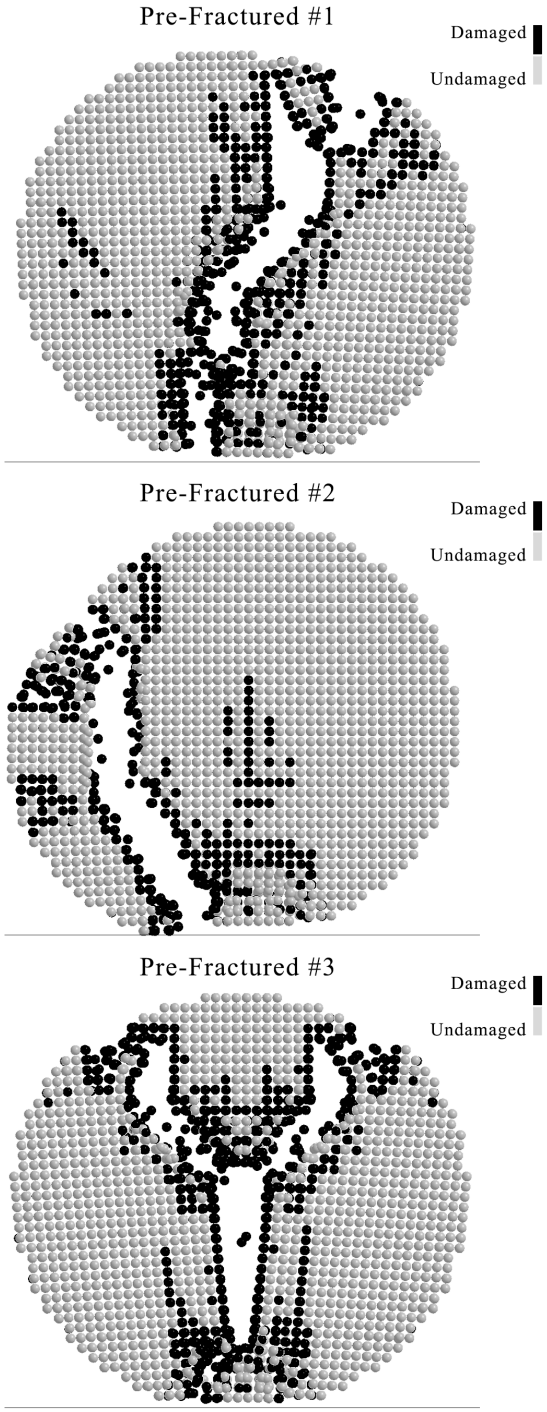

Fig. 13. The deformation of the pre-fractured models with plotted damage.

The article also describes an application of the algorithm for the needs of simulations of a material with initial failure. As it is often very problematic to implement initial material failure within SPH simulations, so the ability of the algorithm to perform this can be considered another important advantage. However, particles with very low or zero mass can pose a problem.

The combination of such singularities with tensile instability can result in the disintegration of the calculation. Also, setting up the interaction (or coupling) with other methods, e.g. FEM, can be problematic.

The entire principle is presented using a simple fracture mechanics test where a concrete cylinder strikes a rigid surface; the results clearly point to the functionality of the algorithm.

In subsequent research, the authors would like to investigate the generation of random fields with predefined distribution functions which are variable in time. This would make it possible to consider phenomena related to the ageing of materials, potentially even with their cyclic loading.

Acknowledgement
This outcome has been achieved with the financial support of project GACR 14-25320S "Aspects of the use of complex nonlinear material models" provided by the Czech Science Foundation; with the support of the project FAST-J-16-3684 "Use of particle models in concrete dynamic stress simulations" provided by the Brno University of Technology fund for specific university research; and also with the support of the project LO1408 "AdMaS UP – Advanced Materials, Structures and Technologies" provided by the Ministry of Education, Youth and Sports under the "National Sustainability Programme I".

References:

[1] Z. Kala, Sensitivity and Reliability Analyses of Lateral-torsional Buckling Resistance of Steel Beams, *Archives of Civil and Mechanical Engineering*, vol. 15, no. 4, 2015, pp. 1098-1107.

[2] Z. Kala, Influence of Partial Safety Factors on Design Reliability of Steel Structures - Probability and Fuzzy Probability Assessments, *Journal of Civil Engineering and Management*, vol. 13, no. 4, 2007, pp. 291-296.

[3] Z. Kala, J. Kala, M. Skaloud, B. Teply, Sensitivity Analysis of the Effect of Initial Imperfections on the (I) Ultimate Load and (II) Fatigue Behaviour of Steel Plate Girders, *Journal of Civil Engineering and Management*, vol. 11, no. 2, 2005, pp. 99-107.

[4] J. Kralik, Safety of Nuclear Power Plants under the Aircraft Attack, *Applied Mechanics and Materials*, vol. 617, 2014, pp. 76-80.

[5] J. Kralik, M. Baran, Numerical Analysis of the Exterior Explosion Effects on the Buildings with Barriers, *Applied Mechanics and Materials*, vol. 390, 2013, pp. 230-234.

[6] J. Kralik, Optimal Design of NPP Containment Protection Against Fuel Container Drop, *Advanced Materials Research*, vol. 688, 2013, pp. 213-221.

[7] P. Kral, J. Kala, P. Hradil, Verification of the Elasto-Plastic Behavior of Nonlinear Concrete Material Models, *International Journal of Mechanics*, vol. 10, 2016, pp. 175-181.

[8] J. Kala, M. Husek, Useful Material Models of Concrete when High Speed Penetrating Fragments are Involved, *Proceedings of the 9th International Conference on Continuum Mechanics*, vol. 15, 2015, pp. 182-185.

[9] F. Hokes, J. Kala, O. Krnavek, Nonlinear Numerical Simulation of a Fracture Test with Use of Optimization for Identification of Material Parameters, *International Journal of Mechanics*, vol. 10, 2016, pp. 159-166.

[10] J. Kala, P. Hradil, M. Bajer, Reinforced concrete wall under shear load – Experimental and nonlinear simulation, *International Journal of Mechanics*, vol. 9, 2015, pp. 206-212.

[11] J. Kala, M. Husek, High Speed Loading of Concrete Constructions with Transformation of Eroded Mass into the SPH, *International Journal of Mechanics*, vol. 10, 2016, pp. 145-150.

[12] J. Kala, M. Husek, Improved Element Erosion Function for Concrete-Like Materials with the SPH Method, *Shock and Vibration*, vol. 2016, 2016, pp. 1-13.

[13] G. R. Liu, M. B. Liu, *Smoothed Particle Hydrodynamics: a meshfree particle method*, World Scientific Publishing Co. Pte. Ltd, 2003.

[14] W. Benz, Smoothed particle hydrodynamics: a review, *NATO Workshop*, Les, Arcs, France; 1989.

[15] Livermore Software Technology Corporation (LSTC), *LS-DYNA Theory Manual*, LSTC, Livermore, California, USA, 2016.

[16] Y. D. Murray, *User's manual for LS-DYNA concrete material model 159*, FHWA-HRT-05-062, 2007.

[17] Y. D. Murray, A. Abu-Odeh, R. Bligh, *Evaluation of concrete material model 159*, FHWA-HRT-05-063, 2006.

[18] M. Husek, J. Kala, P. Kral, F. Hokes, Effect of the Support Domain Size in SPH Fracture Simulations, *International Journal of Mechanics*, vol. 10, 2016, pp. 396-402.